

Modeling and Simulation of Nanoindentation

SIXIE HUANG¹ and CAIZHI ZHOU

1.—Department of Materials Science and Engineering, Missouri University of Science and Technology, Rolla, MO 65409, USA. 2.—Department of Mechanical and Aerospace Engineering, Missouri University of Science and Technology, Rolla, MO 65409, USA. 3.—e-mail: zhouc@mst.edu

Nanoindentation is a hardness test method applied to small volumes of material which can provide some unique effects and spark many related research activities. To fully understand the phenomena observed during nanoindentation tests, modeling and simulation methods have been developed to predict the mechanical response of materials during nanoindentation. However, challenges remain with those computational approaches, because of their length scale, predictive capability, and accuracy. This article reviews recent progress and challenges for modeling and simulation of nanoindentation, including an overview of molecular dynamics, the quasicontinuum method, discrete dislocation dynamics, and the crystal plasticity finite element method, and discusses how to integrate multiscale modeling approaches seamlessly with experimental studies to understand the length-scale effects and microstructure evolution during nanoindentation tests, creating a unique opportunity to establish new calibration procedures for the nanoindentation technique.

INTRODUCTION

With the advancement of atomic force microscopy and other instruments, $^{1-3}$ nanoindentation has become one of the commonest techniques for quantitative characterization of the mechanical properties of materials and has provided some unique effects that have sparked many related research activities. 4,5 To fully understand the phenomena observed during nanoindentation tests, modeling and simulation methods have been developed or utilized to predict the mechanical response of materials during nanoindentation. This review discusses the recent development and remaining challenges for each computational approach and proposes one multiscale modeling approach for nanoindentation, which can help understand the length-scale effects and microstructure evolution during nanoindentation tests.

ATOMISTIC MODELING

Atomistic simulation is one of the most powerful computational methods for modeling and predicting material behavior at the nanoscale. Only relying on interatomic potentials, atomistic simulations can provide valuable insights into the deformation behavior of materials during nanoindentation. Landman et al.⁶ and Hoover et al.⁷ were the pioneers in atomistic simulation of nanoindentation. Landman's work revealed that the jump to contact (JC) phenomenon during indentation is associated with tip-induced sample deformation at about 4.2 Å, which induces pile-up atomic configurations around the edges of the indenter. Hoover's work revealed that the predicted hardness was strongly influenced by the atomistic potential, temperature, and indenter speed used in their simulations. To understand the microstructure evolution below the indenter, Kelchner et al.⁸ developed an effective method, i.e., centrosymmetry parameter analysis, to describe the state of atoms in their simulation results. Later on, researchers performed simulations to investigate the early stages of plasticity during nanoindentation^{9–13} or the local stress for homogeneous nucleation of dislocations by taking advantage of such centrosymmetry parameter analysis. 14,15 Based on knowledge gained from such simulations, the early stage of plasticity in single-crystalline materials was identified during nucleation of dislocations and their subsequent activity, as illustrated in Fig. 1. Dislocation loops that nucleate below the indenter may cross-slip and intersect with each other to form sessile tetrahedral locks that lead to strain

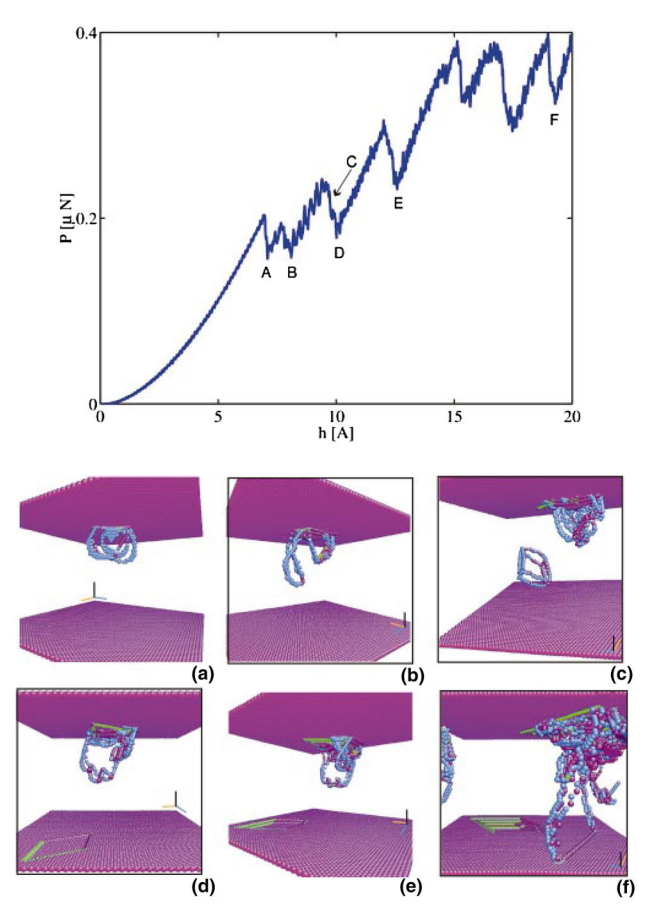


Fig. 1. Correlation of nanoindentation response and atomistic activity in Al during atomistic simulations. The top figure shows the force–displacement curve, while those at the bottom show the corresponding atomistic structure during the indentation process: (a) internal defect structure subsequent to homogeneous nucleation event, (b) expansion of glide loops on the plane, (c) intersection of different glide loops and a sessile lock formed when two loops on different planes intersect, (d) formation of prismatic loop by pinching of stacking fault at four vertices, (e, f) formation of more prismatic loops;¹³ Perfect FCC atoms are set to be invisible.

hardening and motivate nucleation of secondary dislocations. As more dislocations nucleate beneath the indenter, they may pile up at the boundary between the tested material and substrate, which induces large back-stress on the forthcoming dislocations and causes strain hardening during plastic flow. ¹³

Pop-in is a unique phenomenon appearing during nanoindentation and normally indicates sudden release of elastic energy by local plastic deformations. For single crystals, pop-in is related to homogeneous nucleation of dislocations under the indenter. Gouldstone et al. ¹⁶ employed a concise two-dimensional (2D) bubble raft model to simulate homogeneous nucleation of dislocation dipoles and estimated the local stress for homogeneous nucleation to be about $G/2\pi$, where G is the resolved shear modulus. ¹⁷ Because of its ultrahigh critical stress, homogeneous nucleation is less preferred than nucleation of dislocations from or near other

defects, such as grain boundaries (GBs), heterogeneous interfaces, and vacancies. ^{18–22} In their simulations of nanocrystalline Au, Ma et al.²⁰ observed that partial dislocations nucleated from GBs underneath the indenter. On the other hand, Feichtinger et al. 19 demonstrated that dislocations emitted below the indenter can be absorbed by GBs for samples with 5-nm and 12-nm grains. Moreover, Jang et al.²³ visualized that lattice dislocations were transmitted across symmetric tilt GBs and left a step in the boundary plane. Besides GBs, nanoindentation simulations have also been used to explore the deformation mechanism in multilayer metallic (NMM) composites, whose unique properties are attributed to the heterogeneous interfaces between phases. Shao performed a series of simulations on Cu-Nb and Cu-Ni NMM composites (Fig. 2),²⁴⁻²⁸ revealing that the maximum strength of NMM composites is higher than either of the two pure materials. They also found that both interface types and layer thicknesses play important roles in the mechanical behavior of NMM composites. In terms of point defects, the simulations of Njeim et al.²⁹ revealed that the load for onset of plasticity decreased with increasing vacancy concentration and suggested that experimental studies should pay more attention to the influence of vacancies on the mechanical response of materials nanoindentation.

Apart from such fundamental analysis of nucleation strength and sites, atomistic simulations have also been used to explore factors affecting nanoindentation test results. In their simulations, Zhang et al.³⁰ assessed subsurface damage induced by nanomachining and claimed that the hardness of machining materials is insensitive to machining depth, while the critical strength for dislocation nucleation decreases with increasing machining depth. Zimmerman et al.³¹ used the slip vector calculated from their simulations to describe the dislocation nucleation process and revealed how surface geometry affects the nanoindentation results. Sun et al.³² evaluated the effect of residual stress on the mechanical response of materials under nanoindentation. Their simulation results revealed that the residual stress may change the dislocation nucleation site and its slip direction, and the indentation hardness increased with moderate compressive residual stress but decreased under higher compressive residual stress.

Although atomistic simulations can be used to study phenomena observed during nanoindentation, several key challenges remain for this computational method. The first is the length scale of such atomistic simulations. The radius of indenters in simulations is only about 10 nm, which is still much smaller than the actual tip radius of indenters used in experimental studies. Although billion-atom simulations are now feasible using large computing clusters, the dimensions of the simulation box are still limited to about 100 nm. In addition, the

2258 Huang and Zhou

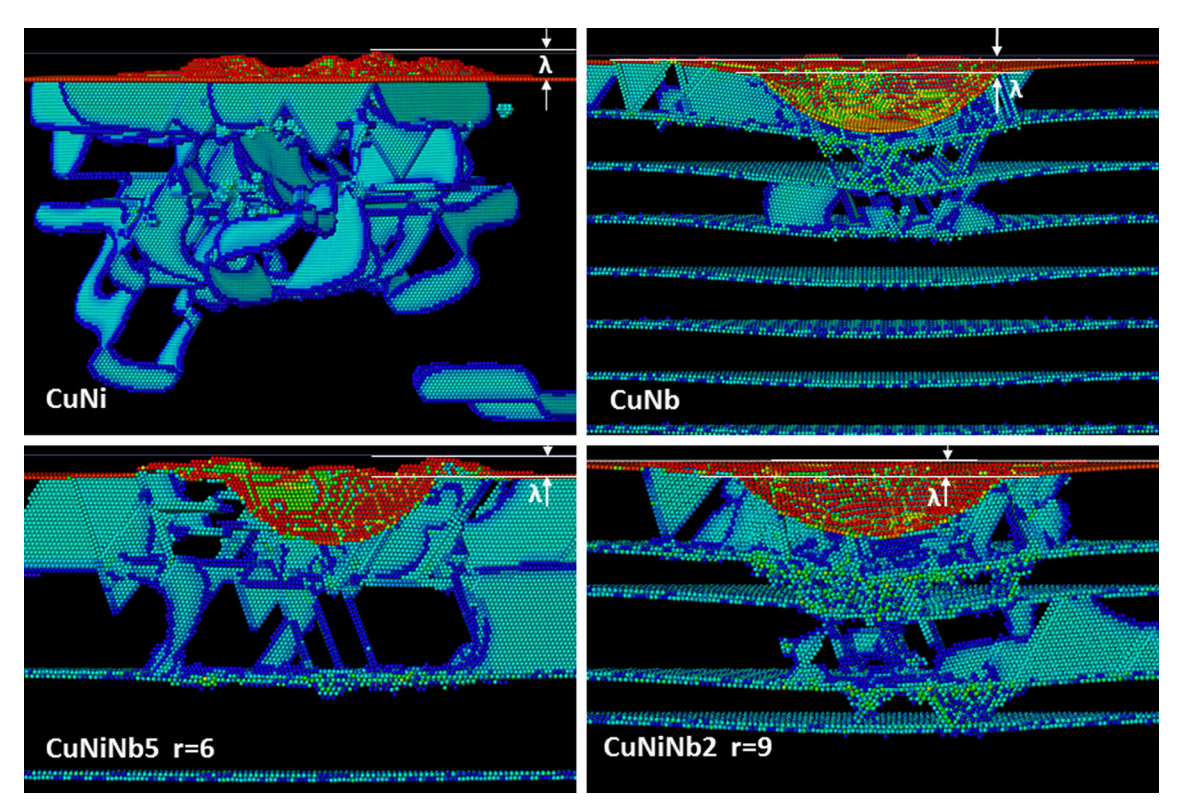


Fig. 2. Surface pile-ups and sink-ins for Cu-Ni, Cu-Nb, and Cu-Ni-Nb multilayers during nanoindentation. The Cu-Ni multilayers tend to have surface pile-ups, while Cu-Nb multilayers tend to have surface sink-ins because the incoherent interface between Cu and Nb phases is stronger than the coherent interface between Cu and Ni phases.²⁷

sample size in atomistic simulations may not be large enough to capture the deformation characteristics of materials with GBs or interfaces. The second challenge is the time scale. Because of the frequency of atomic lattice vibrations, the time interval for simulation steps is often on the picosecond timescale. This short time step forces indenters to move at a rate of about 1 m/s during simulations, which is 1000 times faster than in experimental studies. Theng et al. Conducted several simulations with different loading rates on soft gold and hard diamond and found that the modulus and hardness of both materials varied a lot with loading rate.

Another challenge for atomistic simulations is the interatomic potentials. Atomistic simulations do not require any assumptions except the interatomic potential to predict the activities of atoms. However, the accuracy of the interatomic potential is critically important since it determines all the material properties and simulation results. Simulations using realistic potentials require too much computational resources and time. Empirical interaction potentials, such as the Lennard-Jones (LJ), ³⁵ Tersoff, ³⁶ and Brenner ³⁷ potentials or the embeddedatom method (EAM), ³⁸ have been developed and proven to be efficient for atomistic simulations even with more than ten million atoms. For metallic systems, simple pairwise potentials are not as good as many-body potentials, since pairwise potentials

do not account for the directional nature of bonds nor the environmental dependence. Ziegenhain et al. ³⁹ compared the mechanical properties of Cu as predicted by using pair versus EAM potentials, and found that the pair potential could not predict the elastic anisotropy of cubic crystals and underestimated the stable stacking fault energy. However, when one system contains both metallically and covalently bonded elements such as Ni and Si, the simple pairwise potential is still needed to describe the interactions between atoms. For Ni thin film attached to Si substrate, Yaghoobi et al. ⁴⁰ incorporated Tersoff and LJ potentials into their calculations to simulate the mechanical response of Ni thin film.

A large number of interatomic potentials were developed early on for metallic materials such as Cu, Ni, and Au. ^{6,7,19} Over the past decade, interatomic potentials for nonmetallic systems, such as ceramics and polymers, have been developed and promoted atomistic simulations of those material systems. ^{41–46} Szlufarska et al. ⁴¹ identified that the amorphization of silicon carbide (SiC) during nanoindentation was induced by coalescence of dislocation loops generated below the indenter. The amorphization phenomenon in ceramics was also observed in simulations of silicon nitride (SiN) and molybdenum disulfide (MoS₂) by Walsh et al. ^{42,43} and Stewart et al. ⁴⁴ respectively. In simulations on the MoS₂ system, Stewart found

that the initial amorphization beneath the indenter was induced by intralayer angular bending of S—Mo—S bonds rather than breakage of Mo—Mo or Mo—S bonds, in contrast to the hypothesis proposed based on previous experimental studies. ⁴⁷ In the first nanoindentation simulation of polymers, Pätzold et al. ⁴⁶ identified the characteristic time scale for the dynamics of surface disturbances and damage using free drift simulations, and proposed an effective resistance coefficient to measure the surface hardness. With the development of interatomic potentials for multiple elements, there is a good reason to believe that atomistic simulations of nanoindentation can be extended to more complex material systems.

QUASICONTINUUM METHOD

The quasicontinuum method (QCM) was originally conceived and developed by Tadmor, Ortiz, and Phillips⁴⁸ in 1996, with the goal of modeling an atomistic system without explicitly treating every atom in the problem. In this method, the interatomic potential is directly incorporated into the continuum finite element method via the Cauchy–Born rule to obtain the continuum strain energy density from the energy stored in atomic bonds. Since both discrete atoms and continuum solids are involved in the quasicontinuum method, the method can account for both local and nonlocal effects, ⁴⁹ i.e., multibody atomistic interactions.

Similar to traditional atomistic simulations, most early QCM calculations focused on the initial stages of plasticity during nanoindentation. ^{9,50–53} Smith et al. ⁵⁴ reproduced the experimental force—displacement curves for nanoindentation on Si and observed the microscopic phase transformation during indentation. Both Tadmor ⁵⁰ and Jin ⁵³ found deformation twinning on the (111) indentation surface of pure Al samples (Fig. 3), which did not appear in traditional atomistic simulations of deformation of bulk Al. ⁵⁵

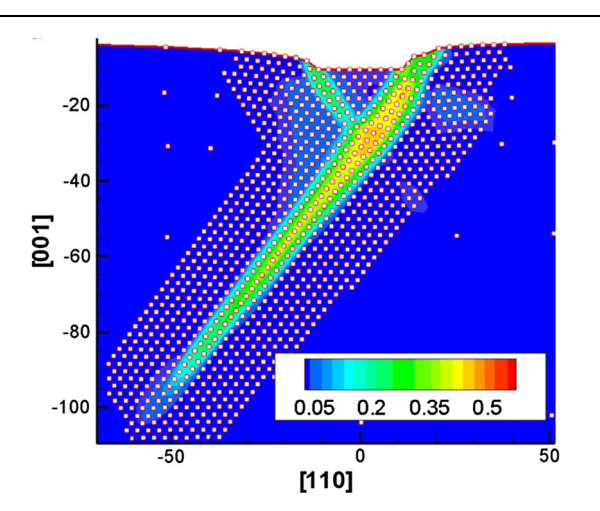


Fig. 3. Contour plot of von Mises strain distribution for indentation depth of 10.5 Å. A single twin with "lens-shaped" structure along the right-hand side of the wedge is shown in the plot.⁵³

QCM calculations were also conducted to explore the effects of sample size, indenter size, tip position, surface roughness, and surface step on nanoindentation results. $^{56-63}$ Although computational analyses using the QCM incorporate multiple length scales to approach realistic dimensions, the conjugate gradient method used in quasicontinuum analysis 64 is an $\rm O(N^2)$ method and therefore not suitable for large problems. In addition, it is hard to eliminate the spurious force appearing at the interface between the domains of the (local) continuum and (nonlocal) atomistic simulations in the quasicontinuum method. 49

DISCRETE DISLOCATION DYNAMICS SIMULATIONS

As a microscale method, discrete dislocation dynamics (DDD) simulations can be used to simulate the motion, multiplication, and interaction of discrete dislocations during plastic deformation. 65–67 DDD simulations, in which dislocations are the simulated entities, offer a way to extend time and length scales beyond those of atomistic simulations. They have been developed to date following the same general procedures: dislocation lines are modeled by placing nodes along the dislocation; the net Peach–Koehler forces on dislocation nodes are determined by summing the stresses from all sources; the equations of motion for the dislocations are then solved for a given time step, and finally the positions are updated. 68–71

To better understand how an indent-induced plastic zone forms, Fivel et al.⁷² performed the first DDD simulation on nanoindentation, in which the finite element method (FEM) elastic solution enforcing the boundary conditions was superimposed onto the infinite medium elastic solution of the discrete dislocations. The plastic deformation was modeled by relaxing the elastic loading stresses through both introduction of new nucleated discrete dislocations (loops) and their motion within the sample. Their DDD simulation results were validated by a nanoindentation test on a (001) copper single crystal. Following that, Rathinam et al. investigated the temperature-dependent behavior of materials during nanoindentation by DDD simulations. They attributed the load drop for smaller indentation depth at higher temperatures to increased dislocation mobility and reduced dislocation density. Tsuru et al. ⁷⁴ developed an integrated computational framework for modeling nanoscale incipient plastic deformation during nanoindentation. In their work, the DDD model combined with boundary element analysis was constructed to capture the collective motion of the dislocations shown in Fig. 4. Their simulation results suggested that the critical shear stress to trigger incipient plastic deformation was much higher than the theoretical shear strength because of the high compressive stress distribution

2260 Huang and Zhou

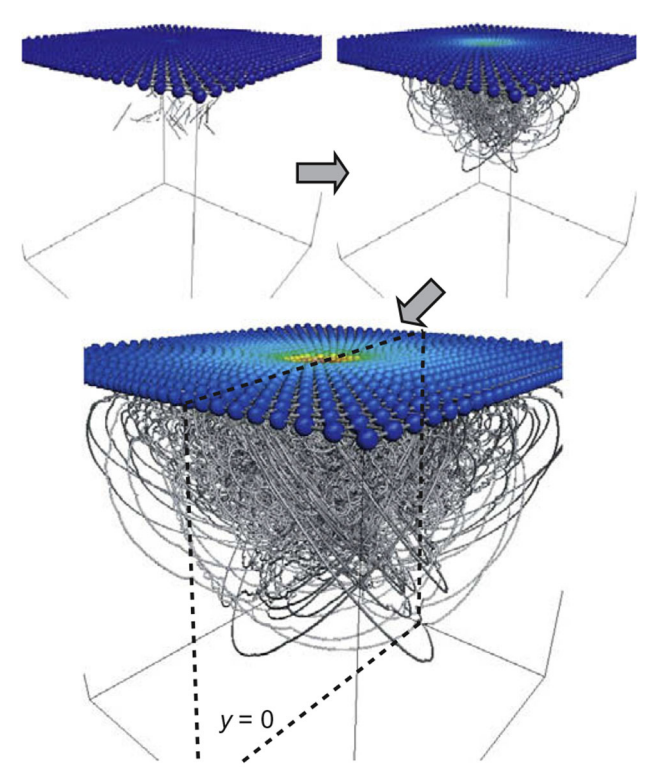


Fig. 4. Overview of a dislocation avalanche under indentation in DDD simulations. The dislocation lines are shown below the atomistic plane, and the displacement field on the surface obtained by solving the boundary integral equation is also visualized.⁷⁴

beneath the indenter, and the displacement burst was induced by surface rearrangement corresponding to hundreds of dislocation dipoles. Although the ad hoc assumptions for the dislocation nucleation process make the information gained from DDD simulations less valuable than atomistic simulations, especially for the initial plasticity during nanoindentation, DDD simulations can still provide useful insights into the evolution of the microstructure in the post-yielding regime, which can enrich the content of computational methods at longer length scales.

CRYSTAL PLASTICITY FINITE ELEMENT METHOD

The crystal plasticity finite element method (CPFEM) was first introduced by Peirce et al. 75 to study the deformation behavior and predict the mechanical response of crystalline materials. CPFEM is a full-field model satisfying both strain compatibility and stress equilibrium. 76 Unlike mean-field crystal plasticity models, CPFEM can assess compatibility at grain/phase boundaries, satisfy local stress equilibrium, and allow for heterogeneities in stress and strain from grain to grain or phase to phase. When applied to nanoindentation, CPFEM calculations allow one-to-one

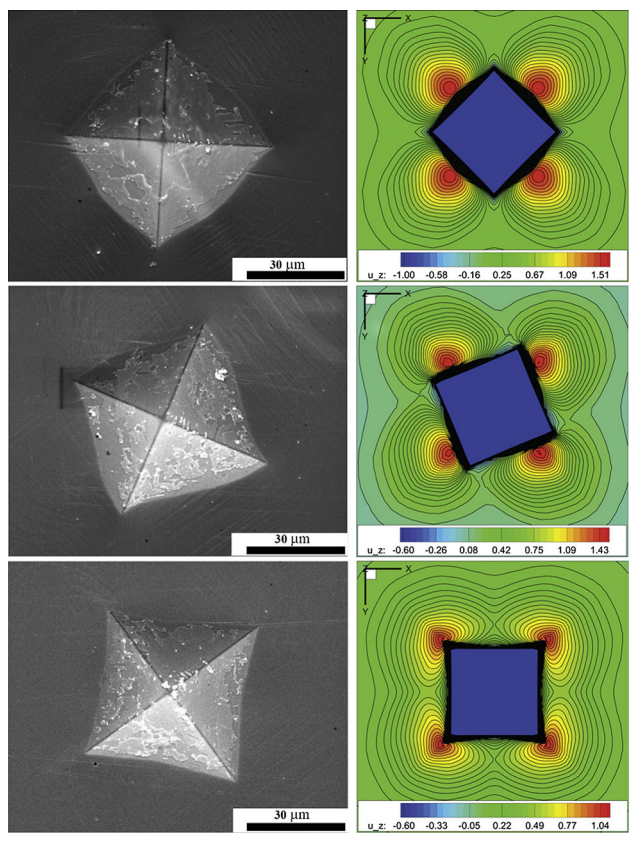


Fig. 5. Comparison of experimental and simulation results of pyramidal indentation into (001) CMSX-4 material, a two-phase Ni-base superalloy. Left: scanning electron microscopy (SEM) images; right: simulation results with isolines of height, u_z (μ m), for azimuthal orientation angle $\emptyset=0^\circ$, 22.5°, and 45° in row 1–3. Both experiment and simulation show that the crystallographic pile-up topography is constantly maximum in the (110) direction, independent of the azimuthal orientation of the indenter. Big 100 microscopy (SEM) images; right: simulation results with a simulation of the indenter.

comparisons of force—displacement curves and remaining imprint topologies generated from modeling and experimental studies to reveal the plastic deformation mechanisms under the indenter.

Early CPFEM works focused on studying the effect of indenter properties such as shape and size, and spherical or conical indenters were used in most simulations due to their higher order symmetry. 77-82 Nix et al. 78 studied the effect of indentation size using a conical indenter by introducing the concept of geometrically necessary dislocation (GND). Qu et al. 79 also investigated the effect of indentation size using a spherical indenter based on the mechanism-based strain gradient plasticity and claimed that indenter geometry had a strong effect on indentation hardness. After those works, several groups performed calculations on Vickers and Berkovich indenters, predicting hardness values, pile-up patterns, and force-displacement curves that matched well with experimental results. Eidel et al.⁸³ explored the size effect of pyramidal indentation on single-crystal Ni-base superalloy. They found that the pile-up and stress concentrations

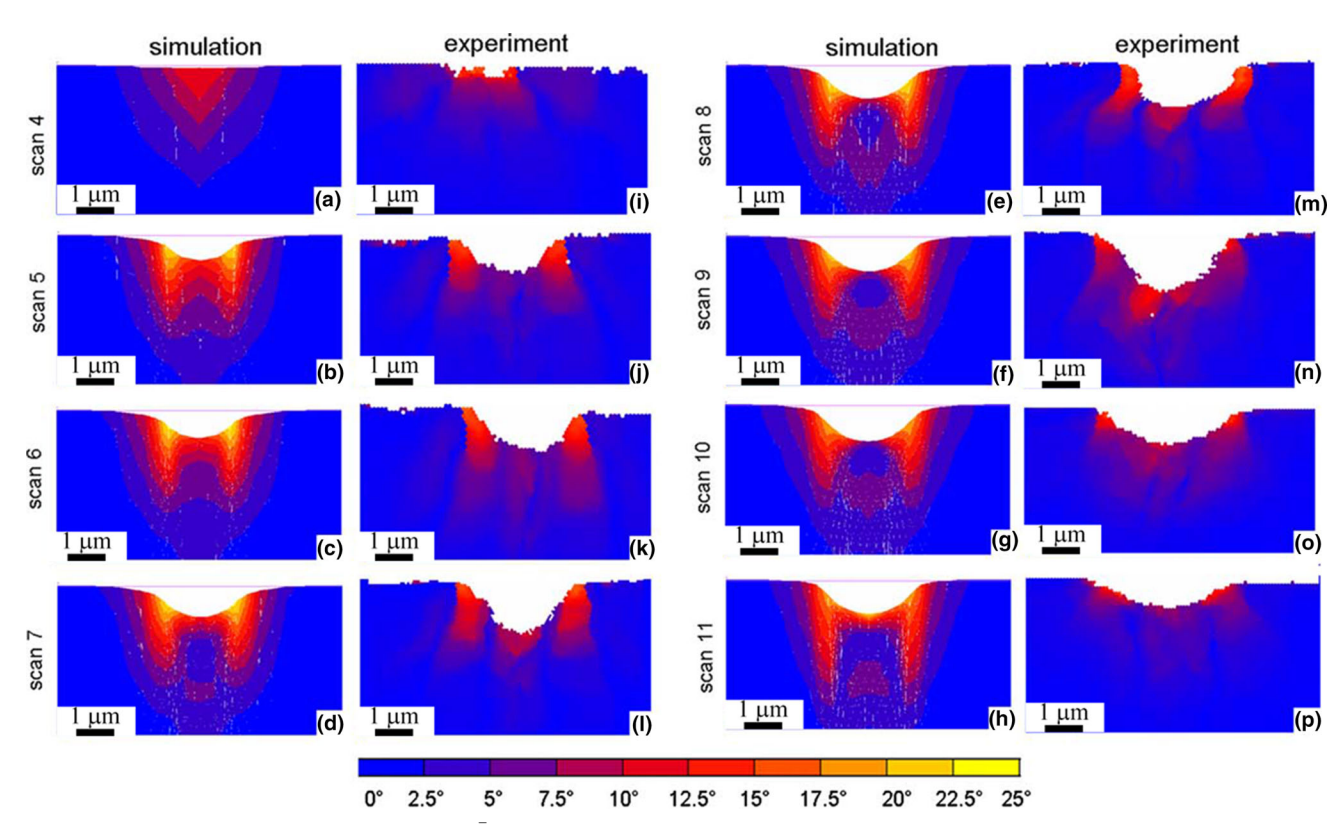


Fig. 6. Rotation maps for a set of successive (11 $\bar{2}$) sections perpendicular to the (111) indentation plane (surface plane perpendicular to the plane presented) with different spacing to the actual indent. Scan 4 is far away from the indenter tip (1567 nm), while scan 10 is close to it (176 nm). The images on the left-hand side (a–h) were obtained from crystal plasticity simulations. The corresponding maps on the right-hand side (i–p) were determined via EBSD measurements in succeeding planes prepared by serial focused ion beam (FIB) sectioning. The color code shows the magnitude of the orientation change relative to the initial crystal orientation without indicating the rotation axis or rotation direction. Scaling is identical for all diagrams.⁸⁷

introduced by the indenter were insensitive to the shape and azimuthal orientation of the pyramidal indenter but depended on the geometry of the discrete slip systems, as shown in Fig. 5.

Unlike atomistic simulations, the main focus of CPFEM calculations is neither the nucleation process nor the initial plasticity during nanoindentation. Most CPFEM works have explored lattice rotation, texture evolution, and pile-up or sink-in patterns during indentation. ^{3,78,84} Materials with low strain-hardening potential tend to pile up against the indenter, while materials with high strain-hardening potential tend to deform downwards, leading to sink-in patterns. Both pile-up and sink-in patterns are closely related to the slip system and its slip behavior in crystalline materials. Since crystalline orientation strongly affects the operation of slip systems, various CPFEM calculations have addressed the effect of orientation on the pile-up patterns formed during nanoindentation. 82,85,86 Two independent calculations done by Wang et al. and Liu et al. observed that the symmetry of the patterns varied with

crystallographic orientation, as verified experimentally.82,86 Lattice rotation during indentation is another important feature that can be captured by CPFEM calculations. Zaafarani et al.⁸⁷ investigated lattice rotation and texture evolution by incorporating three-dimensional (3D) electron backscatter diffraction (EBSD) technology with CPFEM calculations. Both modeling and experimental results showed similar pattern orientation changes, as shown in Fig. 6, although the simulations overemphasized the magnitude of the rotation field tangent to the indenter relative to that directly below the indenter tip. Liu et al.⁸⁸ developed a CPFEM model to investigate the mechanical properties and microtexture evolution of single-crystal aluminum induced by a sharp Berkovich indenter. They predicted lattice rotation angles accurately, and also calibrated the elastic constraint factor in the relationship between indentation hardness and tensile vield stress.

CPFEM calculations rely on model formulations and their parameters. Similar to the interatomic potential in atomistic simulations, the formulation 2262 Huang and Zhou

in CPFEM calculations determines the deformation mechanism during the simulation. Thus the physical meaning of these model formulations is critically important to CPFEM calculations. To date, various deformation mechanisms for certain materials remain to be fully understood, such as nucleation of deformation twins in hexagonal close-packed materials, making creation of reliable CPFEM models for those materials even more difficult. Furthermore, the effect of interactions between different deformation mechanisms needs to be included with reliable and accurate mechanistic details into CPFEM calculations. These challenges must be recognized and addressed in future development of CPFEM models for nanoindentation.

OUTLOOK

Through the development of computer resources and novel experimental methods, macroscopic and phenomenological descriptions of plasticity are being substituted by multiscale approaches rooted in deeper understanding of microstructure- and defect-level processes that occur during deformation of crystalline materials. Challenges remain in terms of developing models with truly predictive capability for application to nanoindentation due to the complex stress state and local microstructure evolution. By harnessing the power of modeling tools at different length scales, hierarchical multiscale modeling methods represent one promising approach to overcome the barriers to different methods for the study of nanoindentation (Fig. 7), i.e., using molecular dynamics simulations for the nanoscale, dislocation dynamics simulations for the microscale, and crystal plasticity models for the macroscale, to reveal how the mechanical response of a material

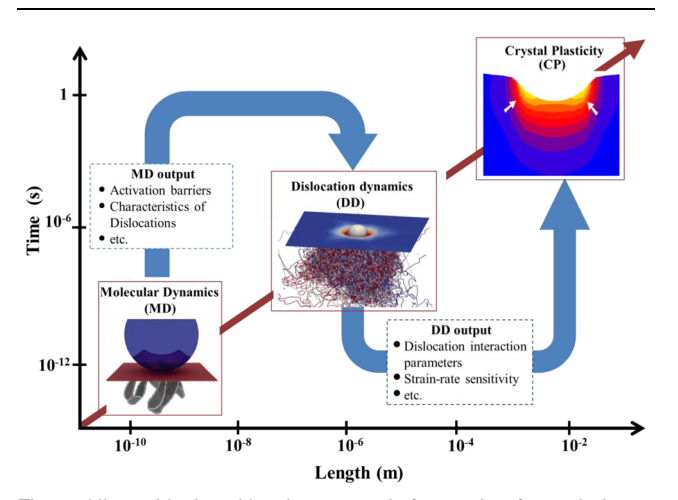


Fig. 7. Hierarchical multiscale approach for study of nanoindentations: bridging the time and length scales by passing information from smaller to larger scales; For instance, results from molecular dynamics (MD) simulations can be imported into dislocation dynamics (DD) simulations, and the results from DD can in turn be imported into a crystal plasticity (CP) model, which can then be used to predict the macroscopic mechanical response of a material during nanoindentation; Inserted modeling figures adapted from Refs. ^{55,87}

during nanoindentation depends on the internal microstructures and associated length scales (grain size and dislocation spacing). This novel multiscale modeling approach can bridge the gap between the atomic and meso/macro scale to study the deformation during nanoindentation at three length scales: atomic, defect, and microstructure.

ACKNOWLEDGEMENTS

This work was supported by an NSF CAREER Award (CMMI-1652662). S.H. is also grateful for partial support provided by The University of Missouri Research Board.

REFERENCES

- W. Gerberich, J. Nelson, E. Lilleodden, P. Anderson, and J. Wyrobek, Acta Mater. 44, 3585 (1996).
- J. Pethicai, R. Hutchings, and W.C. Oliver, *Philos. Mag. A* 48, 593 (1983).
- 3. W.C. Oliver and G.M. Pharr, J. Mater. Res. 7, 1564 (1992).
- 4. G. Pharr and W. Oliver, MRS Bull. 17, 28 (1992).
- B. Bhushan, A.V. Kulkarni, W. Bonin, and J.T. Wyrobek, *Philos. Mag. A* 74, 1117 (1996).
- U. Landman, W. Luedtke, N.A. Burnham, and R.J. Colton, Science 248, 454 (1990).
- W.G. Hoover, A.J. De Groot, C.G. Hoover, I.F. Stowers, T. Kawai, B.L. Holian, T. Boku, S. Ihara, and J. Belak, *Phys. Rev. A* 42, 5844 (1990).
- C.L. Kelchner, S. Plimpton, and J. Hamilton, *Phys. Rev. B* 58, 11085 (1998).
- T. Zhu, J. Li, K.J. Van Vliet, S. Ogata, S. Yip, and S. Suresh, J. Mech. Phys. Solids 52, 691 (2004).
- C. Begau, A. Hartmaier, E.P. George, and G.M. Pharr, *Acta Mater.* 59, 934 (2011).
- G. Ziegenhain, H.M. Urbassek, and A. Hartmaier, J. Appl. Phys. 107, 061807 (2010).
- Y. Lee, J.Y. Park, S.Y. Kim, S. Jun, and S. Im, Mech. Mater. 37, 1035 (2005).
- K.J. Van Vliet, J. Li, T. Zhu, S. Yip, and S. Suresh, *Phys. Rev. B* 67, 104105 (2003).
- R.E. Miller and A. Acharya, J. Mech. Phys. Solids 52, 1507 (2004)
- (2004). 15. R.E. Miller and D. Rodney, *J. Mech. Phys. Solids* 56, 1203
- (2008).16. A. Gouldstone, K.J. Van Vliet, and S. Suresh, *Nature* 411, 656 (2001).
- A. Gouldstone, H.-J. Koh, K.-Y. Zeng, A. Giannakopoulos, and S. Suresh, *Acta Mater.* 48, 2277 (2000).
- 18. K.J. Van Vliet, S. Tsikata, and S. Suresh, Appl. Phys. Lett.
- 83, 1441 (2003).
 19. D. Feichtinger, P. Derlet, and H. Van Swygenhoven, *Phys.*
- Rev. B 67, 024113 (2003).
 20. X.-L. Ma and W. Yang, Nanotechnology 14, 1208 (2003).
- 21. J.H. Yoon, S.J. Kim, and H. Jang, in *Materials Science Forum* (Trans Tech Publ) (2004) p. 89.
- A. Hasnaoui, P. Derlet, and H. Van Swygenhoven, Acta Mater. 52, 2251 (2004).
- 23. H. Jang and D. Farkas, Mater. Lett. 61, 868 (2007).
- S.N. Medyanik and S. Shao, Comput. Mater. Sci. 45, 1129 (2009)
- S. Shao and S.N. Medyanik, Mech. Res. Commun. 37, 315 (2010).
- S. Shao and S. Medyanik, Model. Simul. Mater. Sci. Eng. 18, 055010 (2010).
- S. Shao, H. Zbib, I. Mastorakos, and D. Bahr, J. Appl. Phys. 112, 044307 (2012).
- S. Shao, H. Zbib, I. Mastorakos, and D. Bahr, J. Eng. Mater. Tech. 135, 021001 (2013).
- 29. E. Njeim and D. Bahr, Scr. Mater. 62, 598 (2010).
- J. Zhang, T. Sun, A. Hartmaier, and Y. Yan, *Comput. Mater. Sci.* 59, 14 (2012).

- J. Zimmerman, C. Kelchner, P. Klein, J. Hamilton, and S. Foiles, *Phys. Rev. Lett.* 87, 165507 (2001).
- K. Sun, W. Shen, and L. Ma, Comput. Mater. Sci. 81, 226 (2014).
- J. Belak and I. Stowers, Fundamentals of Friction: Macroscopic and Microscopic Processes (Berlin: Springer, 1992), p. 511.
- C.-L. Liu, T.-H. Fang, and J.-F. Lin, Mater. Sci. Eng. A 452, 135 (2007).
- J.E. Jones, Proc. R. Soc. London A Math. Phys. Eng. Sci. 106, 463 (1924).
- J. Tersoff, Phys. Rev. B 37, 6991 (1988).
- 37. D.W. Brenner, Phys. Rev. B 42, 9458 (1990).
- 38. S. Foiles, M. Baskes, and M. Daw, *Phys. Rev. B* 33, 7983 (1986).
- G. Ziegenhain, A. Hartmaier, and H.M. Urbassek, J. Mech. Phys. Solids 57, 1514 (2009).
- M. Yaghoobi and G.Z. Voyiadjis, Comput. Mater. Sci. 95, 626 (2014).
- I. Szlufarska, R.K. Kalia, A. Nakano, and P. Vashishta, Appl. Phys. Lett. 85, 378 (2004).
- P. Walsh, R.K. Kalia, A. Nakano, P. Vashishta, and S. Saini, Appl. Phys. Lett. 77, 4332 (2000).
- P. Walsh, A. Omeltchenko, R.K. Kalia, A. Nakano, P. Vashishta, and S. Saini, Appl. Phys. Lett. 82, 118 (2003).
- J.A. Stewart and D. Spearot, Model. Simul. Mater. Sci. Eng. 21, 045003 (2013).
- V. Mollica, A. Relini, R. Rolandi, M. Bolognesi, and A. Gliozzi, Eur. Phys. J. E 3, 315 (2000).
- 46. G. Patzold, A. Linke, T. Hapke, and D. Heermann, Z. Phys.
- B Condens. Matter 104, 513 (1997).
 47. N. Takahashi, M. Shiojiri, and S. Enomoto, Wear 146, 107
- (1991).48. E. Tadmor, R. Phillips, and M. Ortiz, *Langmuir* 12, 4529
- V. Shenoy, R. Miller, E. Tadmor, D. Rodney, R. Phillips, and M. Ortiz, J. Mech. Phys. Solids 47, 611 (1999).
- E. Tadmor, R. Miller, R. Phillips, and M. Ortiz, *J. Mater. Res.* 14, 2233 (1999).
- 51. R.A. Iglesias and E.P. Leiva, Acta Mater. 54, 2655 (2006).
- 52. Z. Fanlin and S. Yi, *Acta Mech. Solida Sin.* 19, 283 (2006).
- 53. J. Jin, S. Shevlin, and Z. Guo, Acta Mater. 56, 4358 (2008).
- G. Smith, E. Tadmor, N. Bernstein, and E. Kaxiras, *Acta Mater.* 49, 4089 (2001).
- 55. T. Tsuru and Y. Shibutani, Phys. Rev. B 75, 035415 (2007).
- W.-G. Jiang, J.-J. Su, and X.-Q. Feng, Eng. Fract. Mech. 75, 4965 (2008).
- 57. H. Lu and Y. Ni, Thin Solid Films 520, 4934 (2012).
- H. Lu, Y. Ni, J. Mei, J. Li, and H. Wang, Comput. Mater. Sci. 58, 192 (2012).
- 59. W. Yu and S. Shen, Mater. Sci. Eng. A 526, 211 (2009).
- J. Li, Y. Ni, H. Wang, and J. Mei, Nanoscale Res. Lett. 5, 420 (2009).

- 61. H. Lu, J. Li, and Y. Ni, Comput. Mater. Sci. 50, 2987 (2011).
- 62. W. Yu and S. Shen, Comput. Mater. Sci. 46, 425 (2009).
- 63. W. Yu and S. Shen, Eng. Fract. Mech. 77, 3329 (2010).
- L. Shilkrot, W.A. Curtin, and R.E. Miller, J. Mech. Phys. Solids 50, 2085 (2002).
- B. Devincre and M. Condat, Acta Metall. Mater. 40, 2629 (1992).
- H.M. Zbib, M. Rhee, and J.P. Hirth, Int. J. Mech. Sci. 40, 113 (1998).
- A. Arsenlis, W. Cai, M. Tang, M. Rhee, T. Oppelstrup, G. Hommes, T.G. Pierce, and V.V. Bulatov, Model. Simul. Mater. Sci. Eng. 15, 553 (2007).
- C. Zhou, S.B. Biner, and R. LeSar, Acta Mater. 58, 1565 (2010).
- C. Zhou, S. Biner, and R. LeSar, Scr. Mater. 63, 1096 (2010).
- 70. C. Zhou and R. LeSar, Int. J. Plast. 30, 185 (2012).
- S. Huang, J. Wang, and C. Zhou, Mater. Sci. Eng. A 636, 430 (2015).
- M. Fivel, M. Verdier, and G. Canova, *Mater. Sci. Eng. A* 234, 923 (1997).
- M. Rathinam, R. Thillaigovindan, and P. Paramasivam, J. Mech. Sci. Technol. 23, 2652 (2009).
- 74. T. Tsuru, Y. Shibutani, and Y. Kaji, *Acta Mater.* 58, 3096
- 75. D. Peirce, R. Asaro, and A. Needleman, Acta Metall. 30,
- 1087 (1982).76. F. Roters, P. Eisenlohr, L. Hantcherli, D.D. Tjahjanto, T.R.
- Bieler, and D. Raabe, *Acta Mater.* 58, 1152 (2010).
 77. H.-J. Chang, M. Fivel, D. Rodney, and M. Verdier, *C. R. Phys.* 11, 285 (2010).
- 78. W.D. Nix and H. Gao, *J. Mech. Phys. Solids* 46, 411 (1998).
- S. Qu, Y. Huang, G. Pharr, and K. Hwang, Int. J. Plast. 22, 1265 (2006).
- 80. T. Britton, H. Liang, F. Dunne, and A. Wilkinson, *Proc. R. Soc. London A Math. Phys. Eng. Sci.* 466, 695 (2010).
- S. Kucharski, S. Stupkiewicz, and H. Petryk, *Exp. Mech.* 54, 957 (2014).
- Y. Wang, D. Raabe, C. Klüber, and F. Roters, *Acta Mater*. 52, 2229 (2004).
- 83. B. Eidel, Acta Mater. 59, 1761 (2011).
- J. Alcala, A. Barone, and M. Anglada, *Acta Mater*. 48, 3451 (2000).
- X. Qiu, Y. Huang, W. Nix, K. Hwang, and H. Gao, Acta Mater. 49, 3949 (2001).
- Y. Liu, S. Varghese, J. Ma, M. Yoshino, H. Lu, and R. Komanduri, *Int. J. Plast.* 24, 1990 (2008).
- 87. N. Zaafarani, D. Raabe, R. Singh, F. Roters, and S. Zaefferer, *Acta Mater.* 54, 1863 (2006).
- M. Liu, C. Lu, K.A. Tieu, C.-T. Peng, and C. Kong, Sci. Rep. 5, 15072 (2015).
- Y. Liu, N. Li, S. Shao, M. Gong, J. Wang, R. McCabe, Y. Jiang, and C. Tome, Nat. Commun. 7, 11577 (2016).